EXAMINING MORPHOLOGICAL TRANSITIONING IN *Candida albicans* THROUGH THE MODULATION OF *FKH2*

APPROVED BY SUPERVISING COMMITTEE:

_____
Stephen Saville, Ph.D., Chair

_____
Jose Lopez-Ribot, Ph.D.

_____
Floyd Wormley, Ph.D.

Accepted: _____
Dean, Graduate School

DEDICATION

This thesis is dedicated to my husband David Hess, my mother Elizabeth Hinkle, my sisters May Cobb and Beth Matlock, and my father Charles Cobb Jr. Thank you for your love and support of me in all my endeavors.

EXAMINING MORPHOLOGICAL TRANSITIONING IN *Candida albicans* THROUGH THE MODULATION OF *FKH2*

by

SUSAN LEE COBB, B.F.A.

THESIS
Presented to the Graduate Faculty of
The University of Texas at San Antonio
In partial Fulfillment
Of the Requirements
For the Degree of

MASTER OF SCIENCE IN BIOTECHNOLOGY

THE UNIVERSITY OF TEXAS AT SAN ANTONIO
College of Sciences
Department of Biology
December 2010

ACKNOWLEDGEMENTS

I want to especially thank Dr. Sarah S. Bubeck and Christopher G. Pierce for their guidance in all aspects of my research from theoretical understanding, statistics, technical assistance, and editing to their emotional support and friendship. I want to thank Dr. Ian Cleary and Dr. Stephen Saville for providing the technical protocols for my experiments and for the supervision and management of me for the duration of my research. I would also like to thank Dr. Floyd Wormley and Dr. Jose L. Lopez-Ribot for their helpful suggestions and comments. The pSFS2 is a kind gift of Joachim Morschhaüser and pMT3000 is a kind gift of Mark Paget.

December 2010

EXAMINING MORPHOLOGICAL TRANSITIONING IN *Candida albicans* THROUGH THE MODULATION OF *FKH2*

Susan Lee Cobb, M.S.
The University of Texas at San Antonio, 2010

Supervising Professor: Stephen Saville, Ph.D.

Candida albicans, a human pathogenic fungus, has the ability to transition between three principal morphologies in response to environmental cues: yeast, pseudohyphae, and true hyphae. Previous research shows that the yeast-to-pseudohyphae and yeast-to-hyphae transitions are reversible. What is unclear is whether *C. albicans* pseudohyphae must first revert to yeast before becoming hypha. A recent study in this lab with a tetracycline-regulatable *tet-RFG1* strain suggested that pseudohyphal cells revert back to yeast before transitioning to hyphae. *C. albicans* morphological flexibility allows it to persist in a wide range of host niches and the yeast-to-hyphae transition is believed to be a requisite virulence factor. The elucidation of the complex mechanisms behind these transitioning phenomena will hasten our pursuit of more effective drug targets in the treatment of disease.

In this study, we describe the production, characterization, and use of a novel *fkh2*Δ-*tetFKH2* strain to investigate *C. albicans* morphological transitioning. Fkh2p is an important cell cycle transcription factor and the null mutant grows constitutively as pseudohyphae. A single *tet*-regulatable copy of *FKH2* inserted at the RP10 locus allows the tight regulation of *FKH2* expression in the presence or absence of the tetracycline derivative doxycycline. This regulatable allele gives us the opportunity to grow *Candida albicans* as pseudohyphae by depleting *FKH2* and examining hyphal induction as Fkh2p is restored.

TABLE OF CONTENTS

LIST OF TABLES

LIST OF FIGURES

CHAPTER ONE

INTRODUCTION

Candida albicans is a medically important fungus which causes an array of illnesses within humans. *C. albicans* is the root cause of many mucocutaneous infections including oropharyngeal and genitourinary candidiasis (infections of the mouth and vagina), and systemic infections of the bloodstream (1). *Candida* species comprise the fourth-leading cause of nosocomial infections in the United States behind coagulase-negative *Staphylococci, Staphylococci aureus,* and enterococci infections (16). *Candida albicans* accounts for 35% to 56% of the nosocomial infections attributed to *Candida* species (16). Researchers consider *Candida* infections to be an emerging infectious disease because of the increasing duration that immuno-compromised patients must spend in ICUs and tertiary care facilities following transplantation surgeries, HIV-related illnesses, and neutropenic chemotherapy patients. Candidemia, a *Candida* infection of the bloodstream, has attributable mortality rates of up to 47% in adults and 29% in children during treatment in tertiary care centers in the United Sates (32). According to a study involving phone interviews with U.S. women, the annual cost of *Candida*-associated vaginitis was estimated at $1.8 billion in 1995 and could rise to $3.1 billion by 2014 (18).

Candida species are fungi of the Ascomycota phylum, found as a part of the normal human commensal flora. An alternative environmental reservoir has yet to be discovered. Unlike other dimorphic fungi within the Ascomycota phylum such as *Ajellomyces (Histoplasma) capsulatum* which is a mycelium in soil at 25°C and yeast at 37°C, the *Candida* species alternate from yeast at lower temperatures (less than 30°C) to pseudohyphal and hyphal morphologies at 35-37°C (24). Therefore, *Candida albicans* is most accurately described as a pleiomorph

because it alternates between three principal morphologies in response to environmental cues (27, 40, 45). *Candida albicans'* ability to change morphology enables it to proliferate in an array of human host niches and is believed to be a requisite virulence factor (26, 36).

Defining the characteristics of the principal morphologies is particularly important during genetic studies in order to establish the phenotypic consequence of a specific genetic manipulation. *Candida albicans'* three morphologies are yeast, pseudohyphae, and true hyphae. Yeast cells are round to elongated ovals ranging in size from 8-10μm that exhibit asymmetric polarized growth followed by a switch to isotropic growth (7, 27). The polarized growth in emerging yeast daughter cells is directed by a polarisome which is necessary for the delivery of secretory vesicles to the growing bud (14). The nucleus divides across the (mother-daughter) neck and the daughter yeast cell separates from the mother following cytokinesis. Pseudohyphal cell growth initially resembles yeast in that bud emergence is asymmetric mediated by the polarisome and the first nuclear division also occurs across the mother-daughter bud neck (40). However, the mother and daughter cell walls of pseudohyphae remain attached at the site of septation following cytokinesis and at all the following septal junctions in a uni-polar manner (6). The pseudohyphae are ≥3μm wide at the center and taper towards the septal junctions forming their characteristic constrictions (27, 40). Hyphal cells have parallel sided walls with a width of ~2μm and no constriction at the mother bud neck (27, 40). The first nuclear division occurs within the emerging germ tube across the septal junction anywhere from 5-15μm from the mother bud neck (40). In addition to having a polarisome to direct polarized growth, hyphae have a specific organelle called the Spitzenkorper which acts as a secretory vesicle supplier to the elongating tips (14).

Extensive research has established that the transition between the yeast and the two filamentous morphologies is reversible. What remains unclear is whether the pseudohyphae-to-hyphae transition is direct and whether this transition is reversible. There is controversy among *Candida* researchers because some evidence suggests that the three principal morphologies are separate and distinct fates, with other evidence suggesting a morphological continuum. The distinct fate theory relies on evidence that once a cell reaches a certain point in the cell cycle when apical growth switches to isotropic growth, a checkpoint is passed that determines the cell morphology (7, 37). Also, there is genetic evidence which supports the distinct fate theory based on gene sets that are morphology specific --such as those hyphal-specific genes necessary for the proper function and dynamics of the Spitzenkorper (14). Furthermore, there is genetic evidence indicating that the different gene sets of each specific morphology regulate the rate and order of cell cycle events independent of one another (7, 21, 43). The morphological continuum theory relies on evidence that shows cells can be induced to form filamentous morphologies at all stages within the cell cycle and that the pseudohyphal morphology is an intermediate stage in the yeast-to-hyphae transition (3, 11, 21, 44).

The purpose of this study is to further shed some light on the two theories. At this point, it is useful to explore several experiments which support the two conflicting theories. First, an study conducted by Wightman et al. involving P_{MET3}-*HSL*/*Hsl1*Δ and P_{MET3}-*GIN4/Gin4*Δ mutants that grow constitutively as pseudohyphae in the absence of methionine, showed that at high cell densities the pseudohyphae of the *Hsl*Δ mutant revert back to yeast. When these P_{MET3}-*HSL*/*Hsl1*Δ pseudohyphae, grown under yeast growth conditions (YEPD at 3O°C), reverted back to yeast they were then sub-cultured in YEPD plus serum to induce hyphal formation. These yeast cells transitioned directly to hyphae. In this same study, the P_{MET3}-*GIN4*/*Gin4*Δ was grown

to stationary phase and unbudded yeast were then cultured as pseudohyphae for increasing lengths of time under pseudohyphal conditions (*GIN4* repressing medium) and then challenged with serum to form hyphae. These pseudohyphal cells progressively lost their ability to form hyphae proportionate to the length of time they were cultured as pseudohyphae (46). Interestingly, the wild-type controls in this experiment became proportionately unable to form hyphae as well. In addition, a recent study conducted in our lab with a *tet-RFG1*strain showed that pseudohyphal cells challenged to form hyphae revert back to yeast before continuing to hyphae (34). The *tet-RFG1* strain enables the overexpression of *RFG1* from a single *RFG1* allele placed under the control of a *tet*-regulatable promoter at its genomic locus. When grown in the absence of doxycycline, the strain produces a constitutive pseudohyphal phenotype in yeast growth conditions. In this experiment, the *tet-RFG1*strain was first grown overnight in the absence of doxycycline (*RFG1* overexpressed) to produce a 90% pseudohyphal culture and then sub-cultured into RPMI-1640 minus doxycycline (to maintain *RFG1* overexpression) to induce hyphal formation. The results revealed that before transitioning to hyphae the cells first reverted to a 75% yeast culture (Figure 1).

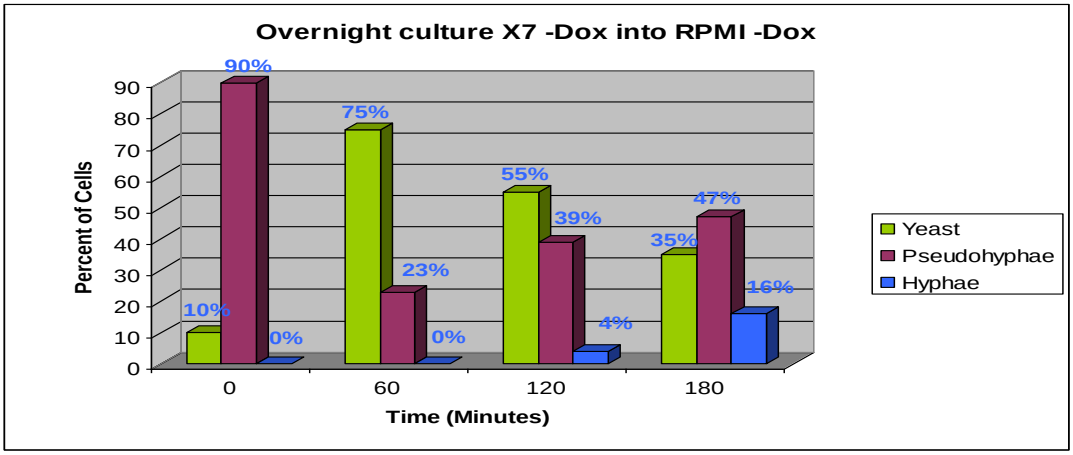

Figure 1: The *tet-RFG1* strain grown overnight minus doxycycline then sub-cultured in RPMI-1640 minus doxycycline to form hyphae (34).

In addition, the proportion of pseudohyphae started to climb again after an initial drop. As we suspected this could be a consequence of conflicting signals: one signal from the *tet-RFG1* overexpression producing the constitutive pseudohyphal phenotype and other signals produced by hyphal induction media. To alleviate this suspicion, the strain was again cultured overnight in YPD minus doxycycline (*RFG1* overexpressed), but this time sub-cultured into RPMI-1640 plus doxycycline which would switch off *tet-RFG1* expression. This removed the conflicting signals and the proportion of pseudohyphae declined throughout the experiment. These results also confirmed that the predominantly pseudohyphal culture reverted to yeast before transitioning to hyphae (Figure 2).

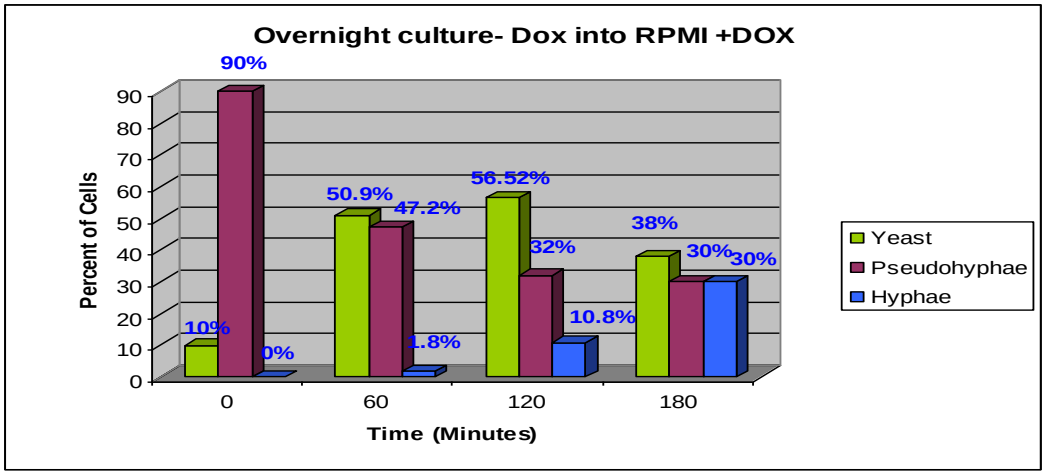

Figure 2: The *tet-RFG1* strain grown overnight minus doxycycline then sub-cultured into RPMI-1640 plus doxycycline and grown at 37°C to form hyphae (34). Note: The equal amounts of pseudohyphal and hyphal morphologies at 180 minutes were due to most of the cells having characteristics of both filamentous morphologies making it difficult to assign them to one group.

Collectively, these results seem to indicate that the yeast morphology is the default starting point for pseudohyphae and that filamentous morphologies are unable to successfully transition from one to another once a commitment point has been reached.

A recent experiment using a *tet-UME6* strain indicated that pseudohyphae can transition directly to hyphae (11). The *tet-UME6* strain allows for the overexpression of *UME6* from one tet-regulatable allele, similar to the case in the *tet-RFG1* strain. The overexpression of *UME6* confers a constitutive hyphal phenotype (2). Carlisle et al. grew the *tet-UME6* strain overnight as yeast in non-filament inducing conditions (YEPD at 30°C) in the presence of doxycycline. These yeast cells were then washed and sub-cultured again into non-filament inducing conditions, but in the absence of doxycycline which allows the overexpression of *UME6*. Cells were visualized at hourly intervals which revealed the gradual transition from yeast-to-pseudohyphae and then from pseudohyphae-to-hyphae. The experiment was then repeated in the opposite direction with a starting culture of constitutive hyphal cells (no doxycycline) and doxycycline was added to a concentration of 40μg/ml. Again, cells show a gradual transition back to yeast with pseudohyphae as an intermediate morphology. The experimental results from the *tet-UME6* strain, suggest that the transitions from yeast-to-pseudohyphae and from pseudohyphae-to-hyphae are not only a continuum, but circuitous. It cannot be ignored that, like the *tet-RFG1*strain experiments, the *tet-UME6* experimental results might be the result of conflicting signals when grown in yeast conditions.

As the previously described experiments have indicated, in order to explore morphological transitioning phenomena it is necessary to develop a strain that will grow constitutively as one morphology when grown under certain conditions, but can still be induced to form others upon growth in a different set of conditions. In this study, we describe the production and utilization

of a new strain in which gene expression can be regulated during morphologic transitioning. First, it was necessary to decide on the appropriate gene to target for manipulation. It was essential that the downregulation or overexpression of the gene produce a constitutive pseudohyphal phenotype and several null mutants are known to do this in *C. albicans*; examples include *hsl1*Δ, *tup1*Δ, *gin4*Δ, *grr1*Δ, *fkh2*Δ, and *clb4*Δ. Hsl1p is the mitotic kinase previously described in the Wightman experiments and is unsuitable due to the pseudohyphae reverting back to yeast at high densities in YPD at 30°C. Tup1p is a transcriptional repressor which is thought to bind Rfg1p and Nrg1p in the repression of hypha-specific genes (8). The fact that Tup1p and Rfg1p are binding partners makes *TUP1* an inappropriate gene to target because results may resemble the previous *tet-RFG1* experiments and be indicative of the disruption of the same filamentation pathway. Gin4p is a mitotic kinase that negatively regulates pseudohyphal formation and null mutants are unable to properly form septin rings making it difficult to definitively distinguish pseudohyphae from hyphae (46). Clb4p, is a mitotic cyclin that must be degraded for mitotic exit which could potentially confer other cell cycle defects during manipulated gene expression (5). Grr1p is a substrate component for the SCF cell cycle ubiquitin ligase and is essential for cell survival and null mutants are unable to utilize certain amino acids (9). Fkh2p is a transcription factor shown to be involved in *Candida albicans* morphogenesis. *FKH2* is not essential for cell growth and survival, but is required for the formation of yeast and true hyphal morphologies (4). Quantitative Real-time PCR analysis conducted on the *tet-RFG1* strain during a previous study in this lab revealed that the *FKH2* transcript level is unchanged during *RFG1* modulation. This indicates that they are in separate, but potentially parallel filamentation pathways (12).

Forkhead proteins, or "winged helix" proteins, are a conserved family of eukaryotic transcription factors (33). In humans, forkhead proteins are associated with cell cycle events (33). The characteristic 110 amino acid DNA-binding motif of forkhead proteins are found within *Candida* species and *Saccharomyces cerevisiae.* These two species diverged ~200 million years ago and are both found within the Ascomycota phylum (8). Extensive genomic analysis of *S. cerevisiae* and *C. albicans* shows that they share highly conserved genes within their regulatory networks (13, 25). In *S. cerevisiae*, there are two redundant Fkh proteins that appear to work in overlapping pathways to regulate cell morphology and separation. The removal of either forkhead gene confers a pseudohyphal phenotype in *S. cerevisiae* (33). Similarly, the single *C. albicans* forkhead protein Fkh2p, is required for the morphogenesis of true hyphal as well as yeast cells and when absent confers a constitutive pseudohyphal phenotype (6). The pseudohyphae of the *fkh2*Δ mutants, like other characteristic pseudohyphal cells, remain attached at the mother-daughter bud neck and fail to separate following cytokinesis (4). The study characterizing Fkh2p in *C. albicans* by Bensen et al. found that this failure to separate was due to Fkh2p positively regulating genes necessary for cell separation: such as *CHT2*, an endochitinase important for yeast cell separation (4). Also, Fkh2p negatively regulates the mitotic B-type cyclin *CLB4* which becomes elevated in *fkh2*Δ null mutants (5). *CLB4* negatively regulates hyper-polarized growth and the elevated *CLB4* in *fkh2*Δ mutants may contribute to their inability to form the hyper-polarization found in true hyphae (5). The same is true in *Saccharomyces cerevisiae,* where Fkh2p is essential for the regulation of cell cycle genes such as *CLB2* and *ACE2*. The scClb2p, like ca*Clb4* is a major mitotic cyclin. The Ace2p in *S. cerevisiae,* is a transcription factor that regulates *CHT1,* encoding an endochitinase similar to caCHT2, necessary for cell separation in yeast cells (15, 23). Finally, the *FKH2* gene was chosen because

the previous study conducted by Bensen et al. using a P_{MET3}-*FKH2/fkh2*Δ strain indicates that it displays the clear phenotypes we need to use as a reference point for the construction of our strain (Figure 3). This study therefore describes the construction, characterization, and use of a novel *tet*-regulatable *FKH2* strain to analyze *C. albicans* morphological transitioning.

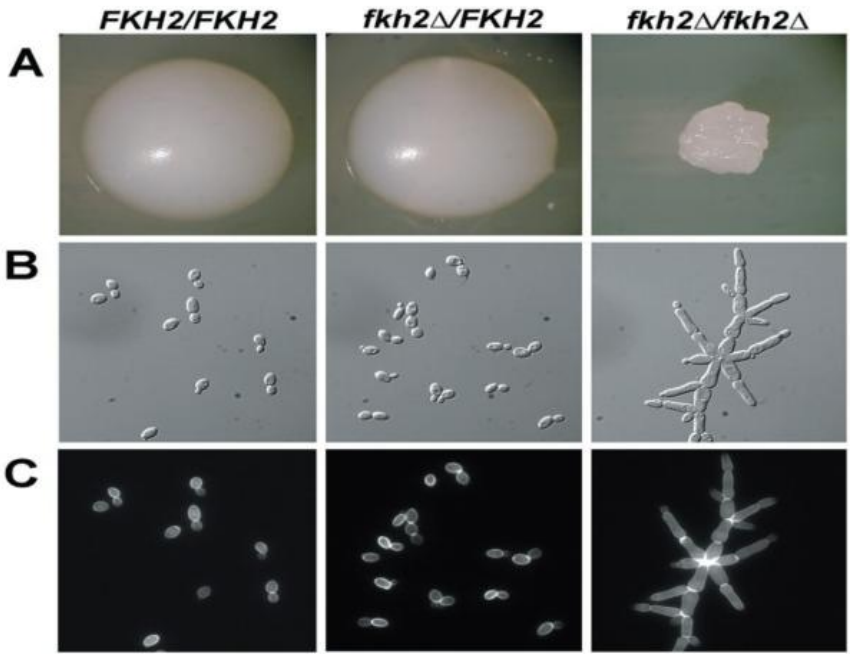

Figure 3: Images by Bensen showing the established phenotypes of *FKH2* mutant strains compared to wild-type strain (4).

CHAPTER TWO

MATERIALS AND METHODS

Strains and media: This study employed the wild-type *C. albicans* strain SC5314 for all genomic amplifications and the TR transactivator gene strain, THE1 (30), as the parent to construct all other strains listed in Table 1. THE1-CIp10, a derivative strain of the parent THE1 containing the *URA3* gene inserted at the RP10 locus (thereby alleviating the uridine auxotrophy), was used for comparative analysis in several experiments (10). All yeast strains were maintained at -80°C as glycerol stocks and grown in yeast extract-peptone-dextrose (YPD) liquid medium at 30°C to maintain a yeast morphology or RPMI-1640 at 37°C for hyphal induction studies. Nourseothricin-resistance selection was achieved by growth on YPD agar containing 200μg/ml while uracil prototrophy transformant selection was achieved on semi-defined (SD) plates lacking uridine. The gene deletion method used in this study requires growth in yeast extract-peptone-maltose (YPM) liquid medium at 30°C to induce the *FLP* recombinase which excises the ~4.2bp *SAT1* flipper cassette between the FRT sites (35). Cells from the YPM cultures were diluted 1/10,000 and plated on YPD agar containing 20μg/ml nourseothricin followed by selection of small colonies which were split and streaked onto YPD agar alone and YPD agar containing 200μg/ml nourseothricin. Sensitivity assays were performed on YPD agar plates plus cell-wall perturbing agents; 0.025% and 0.005% SDS, 100μg/ml Calcofluor White, 200μg/ml Congo Red, 1M $NaCl_2$, or 1M $NaCl_2$ + 1M sorbitol. *Escherichia coli* strain DH5α was utilized for all plasmid manipulations and grown in Luria Broth (LB) medium at 37°C containing 100ug/ml ampicillin as needed to select transformants.

***C. albicans* Electroporation Transformation:** *C. albicans* electroporation transformations were done with an Eppendorf (Hamburg, Germany) electroporator set at 1800V. *Candida* cells were grown to an OD_{600} reading of between 1.2- 2.0 with an optimum reading at 1.6. Cell treatments included incubations periods with 0.01M LiAc and 1X TE at pH7.5 followed by treatment with 0.025M dithiothreitol to increase transformation efficiency (41). After electroporation, cells were plated on SD plates lacking uridine or on YPD plates containing 200μg/ml nourseothricin depending on the selection required.

Southern Blotting: Two separate probe labeling techniques for Southern blotting were used in this study. The first labeling used radioactive ^{32}P-dCTPs to label the *FKH2*-RHF probe and the second using a DIG High Prime DNA Labeling and Detection Kit (Roche, Mannheim, Germany). The first Southern blot was to confirm the flipper cassette integration at one of the THE1 parent genomic loci. The colonies that were nourseothricin resistant were purified using a MasterPure yeast DNA extraction kit (Epicenter Biotechnologies), and digested with HindIII. Digestion reactions were run on a 0.7% agarose gel, denatured, neutralized, and transferred to a positively charged Nytran membrane (Whatman). The DNA was UV cross-linked to the membrane and probed with the *FKH2*-RHF radioactively-labeled with ^{32}P-dCTPs using Ready-To-Go DNA labeling beads (GE Healthcare). The second Southern blot was to confirm the integration of the flipper cassette into the second genomic allele of the newly constructed fkh2Δ/*FKH2-tetFKH2* strain. This Southern followed the same procedure except that the *FKH2*-RHF probe was labeled with the random addition of dioxigenin-dUTPs by a Klenow enzyme. The DIG-system uses an immunoassay based on NBT/BCIP (Nitro-Blue Tetrazolium Chloride/5-Bromo-4 Chloro-3'-Indolyphosphate p-Toluidine salt) cromogenic detection.

Morphological observations and fluorescence microscopy: *Candida albicans* cells were visualized and images captured at 40X and 100X magnification using an epifluoresence microscope (Leica) after staining with Calcofluor white (Sigma) and the use of Vectashield™ mounting medium containing DAPI (Vector Labs, CA). The light microscope images were taken with 100X objective (Fisher Scientific).

TABLE 1: Strains used in this study

Strain	*Genotype*	*Reference*
SC5314	Wild type	(20)
THE1	*ade2*::*hisG/ade2*::*hisG ura3*::*imm434/ura3*::*imm434 ENO1/eno1*::*ENO1-tetR-ScHAP4AD-3HA-ADE2*	(30)
THE1-CIp10 (10)	THE1 with RP10::CIpURA3	
fkh2Δ+*tetFKH2*-10	THE1 with RP10::CIp*tet*O-*FKH2 fkh2*Δ*::FRT/fkh2*Δ*-SAT1-FLP*	This study
fkh2Δ+*tetFKH2*-12	THE1 with RP10::CIp*tet*O-*FKH2 fkh2*Δ*::FRT/fkh2*Δ*-SAT1-FLP*	This study
fkh2Δ+*tetFKH2*-20	THE1 with RP10::CIp*tet*O-*FKH2 fkh2*Δ*::FRT/fkh2*Δ*-SAT1-FLP*	This study
fkh2Δ+*tetFKH2*-29	THE1 with RP10::CIp*tet*O-*FKH2 fkh2*Δ*::FRT/fkh2*Δ*-SAT1-FLP*	This study
fkh2Δ+*tetFKH2*-31	THE1 with RP10::CIp*tet*O-*FKH2 fkh2*Δ*::FRT/fkh2*Δ*-SAT1-FLP*	This study
fkh2Δ+*tetFKH2*-20	THE1 with RP10::CIp*tet*O-*FKH2 fkh2*Δ*::FRT/fkh2*Δ*-FRT*	This study

TABLE 2: Plasmids used in this study

Name	*Reference*
pMT3000	(31)
pSFS2	(14)
CIp10-*tet*O	(unpublished)
pSFS2-*FKH2*-RHF	This study
pSFS2-*FKH2*-LHF	This study
pSFS2-*FKH2*-LHF-RHF	This study
CIpSAT	(12)
pGFP-HIS1	(19)
pGFP-*SAT1*	This study

TABLE 3: PCR primers used in this study

Name	*Sequences ('5-'3)*[a]	*Reference*
FKH2-RHF-DS	GAGCTCGTTCCTAAATCTACCTTTGTCA	This study
FKH2-RHF-UPS	CCGCGGTTTGATACACTTCACTCACACAGA	This study
FKH2-LHFinner-DS	CTCGAGTGGACTTGAATCAAACGTATTT	This study
FKH2-LHFinner-UPS	GGGCCCAAAAACAAAAATCAGCAAACCAA	This study
FKH2-LHFouter-UPS	GGGCCCATTCACGCACTCGTTTTTCC	This study
FKH2-LHFouter-DS	CTCGAGTTGGTTTGCTGATTTTTGTTTTT	This study
FKH2-UPS	CTCGAGAATGTCAGCACAATTTATCACACC	This study
FKH2-DS	AGCTTCCCCTTGGTTATGTTGTTGC	This study
SAT1-FOR	GGGCCCGAATTCGCATGCCAGCGTC	(12)
SAT1-REV	GGGAATTCGATTTCTAGAAGGACCAC	(12)
NOP1-FOR	ACCTTGGAACCTTATGAAAGAGACCATT GTATTGTTGTTGGTAGATACATGAGAAG CGGAATAAAGAAAggtggtggttctaaaggtgaaga attatt	(19)
NOP1-REV	TTTTTAGTTTTCAATAATCAAATGTATTAA TCCTATTGTACAAAATATTTTTATTTAAAA TTTAGAGTATCCC**GATTTCTAGAAGGAC CAC**	(19)
CDC3-FOR	ACAAAAATTATTACCACAAGACCCACCA GCACAACCAGCTCCACAAAAGAGTCGTAA AGGATTTTTACGTggtggtggttctaaaggtgaagaattatt	(19)
CDC3-REV	AATTAAACAAACAGATTAACAAACAAATA AACTAAATTAAGTTACATACTATTTAGCTA TACCTCGGCCC**GATTTCTAGAAGGACCAC**	(19)
PCR-verified insertions:		
URA3-OUT	TGACACCTGGAGTTGGATTAGA	(12)
RP10-IN2	CAAGGTTCCGAAGACCACTC	(12)
Real-time Primers:		
ACT1-S	ATGTGTAAAGCCGGTTTTGCCG	(42)
ACT1-A	CCATATCGTCCCAGTTGGAAAC	(42)
*FKH2*_FOR	GCAAACTCGCTCCAATCAAA	(12)
*FKH2*_REV	TGCTTGCGTAATCATTGTCG	(12)

[a] Underlined sequences are the engineered restriction sites. Uppercase indicates homology to genomic DNA for integrative purposes. Lowercase indicates homology to plasmids described in the work of Gerami-Nejad et al. (19). Uppercase bold indicates *SAT1* homology of newly constructed plasmid.

CHAPTER THREE

RESULTS

Regulatable strain construction: The first step to generating the *tet*-regulatable strain was to develop an *fkh2*Δ/*FKH2* strain. To accomplish this we employed the *SAT1* flipper cassette-based gene knock-out system (35). The ~4.2 kb *SAT1* flipper cassette, contained in pSFS2, has the *C. albicans*-adapted flip recombinase gene (caFLP) and a *C. albicans*-adapted nourseothricin resistance gene (ca*SAT1*) derived from *Streptomyces noursei* (35). The genes ca*FLP* and ca*SAT1*are flanked with 34-bp FRT sites (for the *FLP* recombinase target sequence) (Figure 4). The *SAT1* flipper system utilizes *FLP* recombinase to excise the *SAT1* cassette at the FRT sites. When the cassette is flanked by upstream and downstream sequences of *FKH2*, the *C. albicans* homologous recombination machinery is able to remove each allele from its endogenous loci.

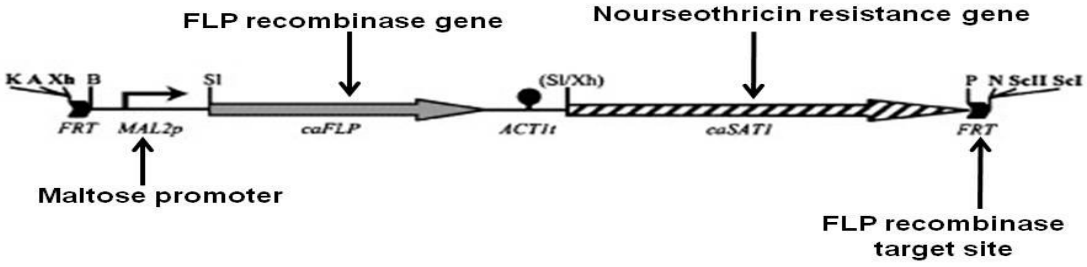

Figure 4: *SAT1* Flipper Cassette (35)

To increase correct enzyme digestion at the restriction sites and subsequently increase ligation efficiency during the incorporation of *FKH2* flanking regions into the plasmid pSFS2 (35). The *FKH2* flanking regions were first cloned into pMT3000 by blunt end ligation (31). This cloning procedure allows the restriction enzymes to cut within the plasmid rather than at the ends of linear PCR products. Furthermore, when the fragment is liberated and purified it easily verifies the fragment's approximate size and concentration for subsequent ligation into the pSFS2 vector. The downstream flanking region (RHF) of *FKH2* was amplified from the genomic DNA of SC5314 using the primers *FKH2*-RHF-UPS and *FKH2*-RHF-DS designed to anneal at the +3154 and +3410 downstream relative to the *FKH2* ORF and engineered to include SacI and SacII restriction sites, respectively (Table 3). The ~500bp PCR product was run on a 1% agarose gel, purified using QIA quick^{TM} gel extraction kit (Qiagen, Valencia, CA), blunt end ligated into SmaI digested pMT3000 (31), and then transformed into *E. coli* strain DH5α. Transformations were plated on LB/Amp/X-gal and screened by blue/white selection. White colonies were cultured overnight in LB containing 100ug/ml ampicillin, 1.5 -3.0 ml of the overnight culture was harvested, and the plasmid DNA isolated using the Wizard DNA Purification Kit (Promega, Madison, WI). Appropriate recombinants (pMT3000-*FKH2*-RHF) were identified via EcoRI digestion and agarose gel electrophoresis. Upon verification, the *FKH2*-RHF insert was liberated by digestion with SacI and SacII and finally ligated between the same sites in the pSFS2 vector to create pSFS2-*FKH2*-RHF. This technique was then repeated using PCR primers *FKH2*-LHFouter-UPS, *FKH2*-LHFouter-DS, *FKH2*-LHFinner-DS and *FKH2*-LHFinner-UPS (restriction sites ApaI and XhoI) for the separate integrations of upstream inner and outer flanking regions into pMT3000 (Table 3). The separate plasmids produced pMT3000-LHFouter and pMT3000-LHFinner were digested and separately integrated into

pSFS2-*FKH2*-RHF to create pSFS2-*FKH2*-LHFinner-RHF or pSFS2-*FKH2*-LHFouter-RHF, respectively. The two plasmids produced with a left-hand inner flank nested inside the left-hand outer flank are necessary to maintain ca*FKH2* endogenous homology for deletion of the second allele. To remove the first allele the parent strain, THE1, was transformed with the *FKH2*-LHFouter-RHF flanked *FLP* cassette which was liberated from the pSFS2 vector. Transformants were identified by plating on YPD plus 200μg/ml nourseothricin which selects for the successful integration of the ca*SAT1* marker gene into THE1 at one of the *FKH2* genomic loci. The *fkh2*Δ/*FKH2* heterozygotes were then confirmed by Southern blot using the PCR amplified *FKH2*-RHF as a probe (Figure 5). Genomic DNA from THE1 and all the potential heterozygotes was digested with HindIII, probed and compared to HindIII digested λ DNA as the molecular marker. We expected to visualize two bands at ~8.6kb and ~6.1kb corresponding to the predicted sizes of the remaining endogenous copy of *FKH2* and the one in which the *FKH2* open reading frame has been replaced with the *SAT1* flipper cassette, respectively. In our blot, we observed the two predicted bands, but also a third hybridizing fragment of ~4.1kb. Since, this is the size expected following the excision of the flipper cassette; we concluded that due to the *MAL2* promoter being leaky we visualized a third band at ~4.1kb where the cassette has already flipped out prior to YPM culturing.

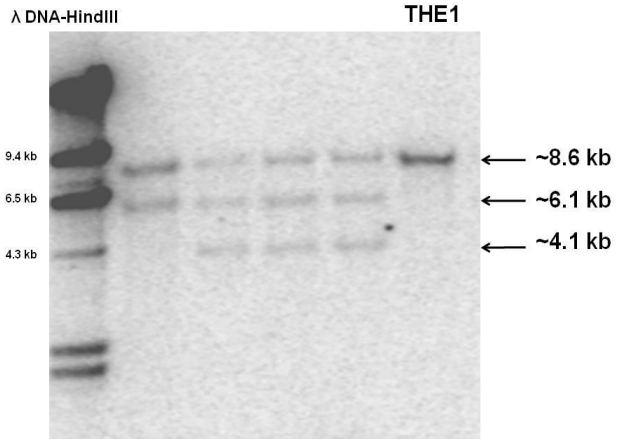

Figure 5: Southern blot confirming the flip cassette integration at of one *FKH2* genomic locus.

To ensure the complete excision of the cassette, the strains were grown in YPM liquid medium to fully express the *FLP* recombinase gene at the *MAL2* promoter.

***Integration of a Tet*-regulatable copy of *FKH2* at the RP10 locus:** The second step in the process of generating the *C. albicans fkh2*Δ+*tetFKH2* strain was to insert a *tet*-regulatable copy of *FKH2* into the RP10 locus of the *fkh*2/*FKH2* heterozygote described above. This was necessary because previous studies have shown that the *FKH2*Δ null mutant grows constitutively as pseudohyphae which have a tendency to flocculate in liquid culture and invade agar plates making handling difficult (4). By inserting the regulatable copy of *FKH2* before deleting the remaining endogenous *FKH2* allele, we were able to alleviate this culturing problem. We employed the tetracycline-regulatable (TR) expression system which allows the tight repression and high fold induction of genes during both *in vitro* and *in vivo* growth (30). The *FKH2* ORF was first amplified from SC5314 genomic DNA using primers *FKH2*-UPS and *FKH2*-DS which incorporated XhoI and HindIII restriction sites at the 5'and 3' ends of the ORF, respectively.

The PCR product was blunt end ligated in to pMT3000 and then transformed into *E. coli* strain DH5α and the resulting pMT3000-*FKH2* was sequenced. Following sequence verification by comparison to the sequence of *FKH2* found within the Candida Genome Database, the *FKH2* was excised using the engineered (XhoI and HindIII) restriction sites and ligated into the CIp10-*tet*O plasmid to generate CIp10-*tet*O-*FKH2*, placing the open reading frame under the control of the *tet*-regulatable promoter. In order to integrate the *tet*O-*FKH2* construct into the *C. albicans* RP10 locus, CIp10-*tet*O-*FKH2* was transformed into the *fkh2*Δ/*FKH2* strain described above. Appropriate integration was confirmed in four individual *fkh2*Δ/*FKH2*+*tetFKH2* isolates using the *URA3*-OUT and RP10-IN2 primers (Table 3) (Figure 6).

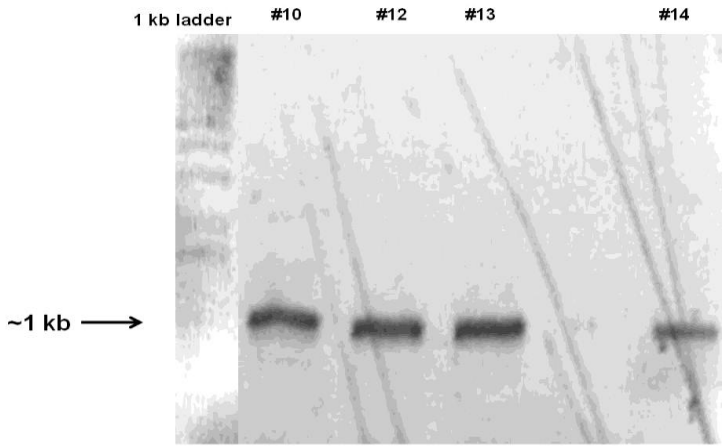

Figure 6: Integration confirmations by PCR amplification of the *URA3* gene and the proceeding section of the RP10 locus, the expected product is 965bp.

To knock-out the second endogenous *FKH2* allele and thus complete the construction of the *fkh2*Δ+*tetFKH2* strain, we used the *FKH2*-LHFinner-RHF flanked *FLP* cassette which was liberated from the pSFS2 vector to transform the confirmed *fkh2*Δ/*FKH2*+*tetFKH2* isolates. Five of the resulting *fkh2*Δ+*tetFKH2* nourseothricin resistant transformants were confirmed by

Southern blot using the PCR amplified *FKH2*-RHF as a probe (Figure 7). Genomic DNA from all of the potential *fkh2*Δ+*tetFKH2* transformants and the THE1 parent were HindIII digested and compared to λ DNA (digested with EcoRI and HindIII). THE1 shows a single ~8.6 kb band corresponding to the endogenous *FKH2*. Isolates 10, 12, 20, 29, and 31 have the two bands (of ~6.1 kb and ~4.1 kb) showing the second *FKH2* allele has been replaced with the *SAT1* flipper cassette and one corresponding to the absence of the first allele, respectively.

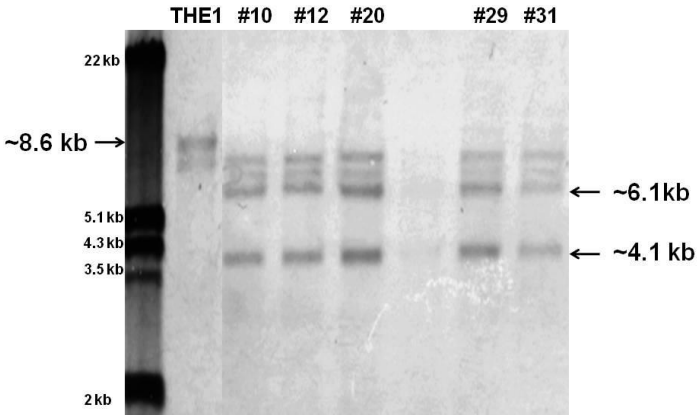

Figure 7: Southern blot confirming *fkh2*Δ+*tetFKH2*

Morphology is determined by doxycycline in the *fkh2*Δ+*tetFKH2* strains under yeast growth conditions: To verify that the *FKH2* regulatable strain would grow as expected we tested the strain under yeast growth conditions (YPD at 30°C) in the presence (20μg/ml) and absence of doxycycline (Figure 8).

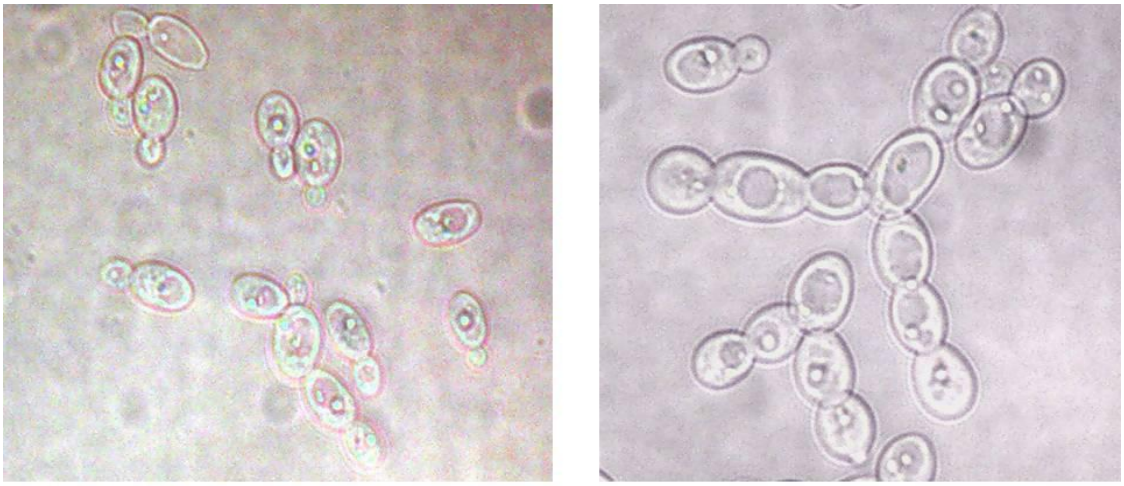

Figure 8: The fkh2Δ+*tetFKH2*-20 strain grown overnight plus and minus doxycycline in YPD at 30°C.

As predicted, the *fkh2*Δ+*tetFKH2*-20 isolate grew as yeast in the absence of doxycycline and as pseudohyphae in the presence of doxycycline.

***In vitro* analysis of the morphological transition from pseudohyphae to hyphae during the modulation of *FKH2* with doxycycline:** To strictly examine the pseudohypha-to-hypha transition, the *fkh2*Δ+*tetFKH2*-29 strain was grown as a 20ml overnight culture for ~22 hours in YPD plus 20µg/ml doxycycline (no *FKH2* expression) to produce the constitutive pseudohyphal phenotype. The following day 1ml was harvested, washed 3X with PBS (phosphate-buffered saline), sub-cultured 1:20 into RPMI-1640 minus doxycycline (induction of *FKH2*) and grown at 37°C for 6hrs. Aliquots (1ml) were collected every 30 minutes for the first two hours and then every hour. The cells were stained with 20µg/ml Calcofluor White for 10 minutes after being washed and resuspended in PBS. Excess Calcofluor White was removed by washing twice in

PBS before the cells were spotted onto a microscope slide and mounted with DAPI containing mounting medium to enable visualization of both morphology and nuclear location. Cell counts were made by examining at least 20 fields of view of epifluoresence images from each time point (n= 3512 cells) (Figure 9).

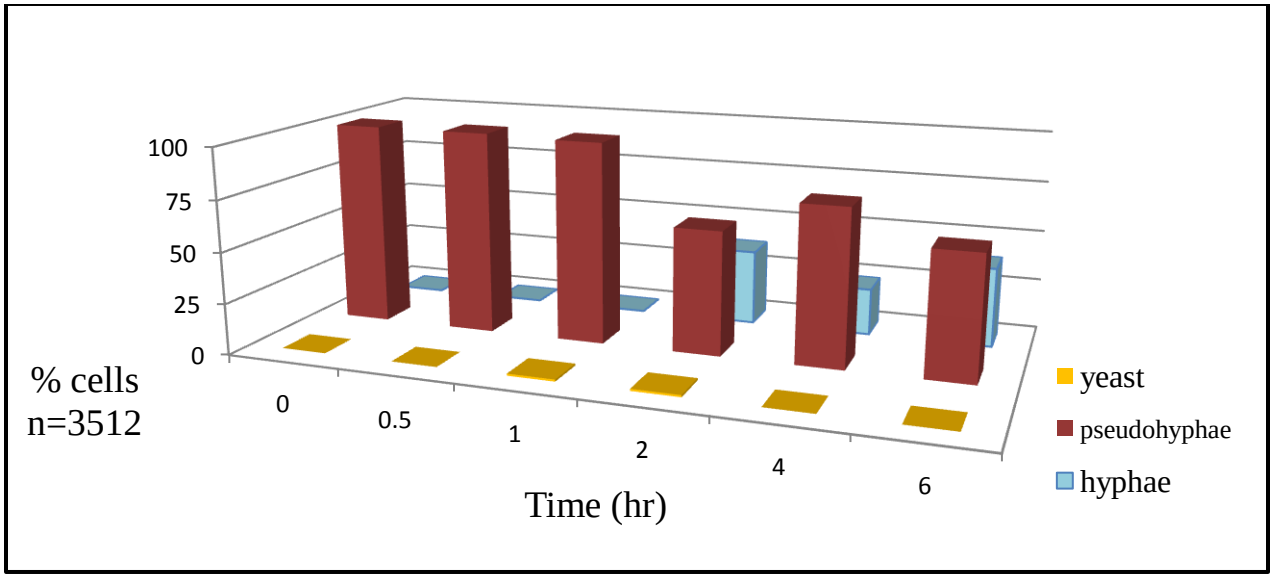

Figure 9: The *fkh2*Δ+*tetFKH2*-29 strain grown in yeast conditions for 22hrs overnight then sub-cultured into RPMI-1640 to induce hyphal formation.

These results show that a 100% pseudohyphal culture of the *fkh2*Δ+*tetFKH2*-29 strain induced to form hyphae does not show a rise in the yeast cell population before transitioning directly to hyphae. To substantiate these results, we repeated the *in vitro* analysis using the *fkh2*Δ+*tetFKH2*-31 strain (n= 1875 cells) (Figure 10).

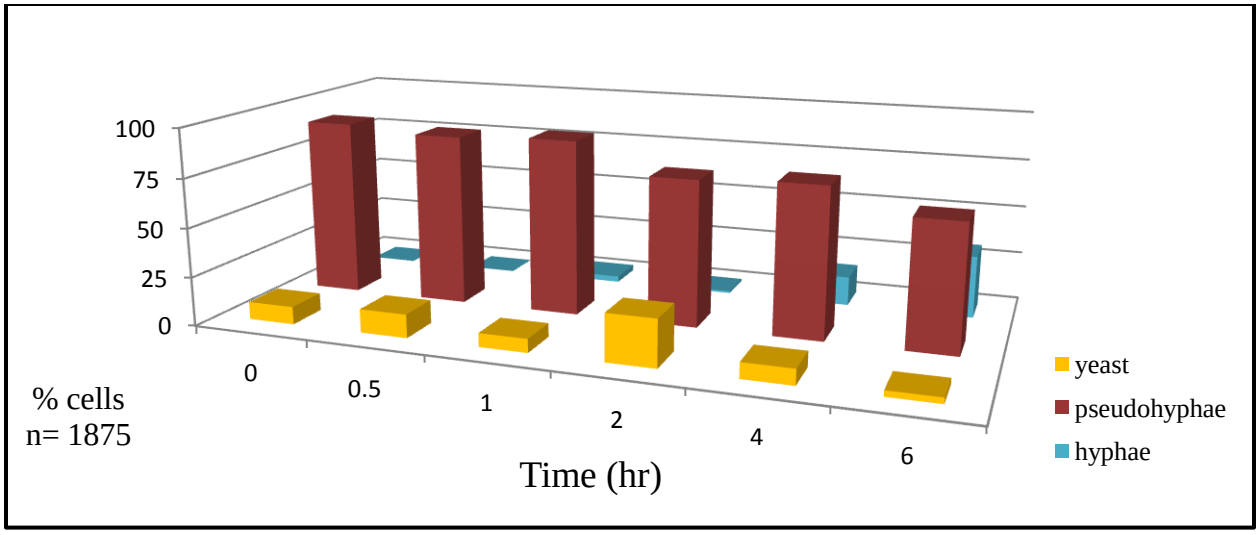

Figure 10: The *fkh2*Δ+*tetFKH2*-31 strain grown in yeast conditions for 18hrs overnight then sub-cultured into RPMI-1640 to induce hyphal formation.

Results from the *fkh2*Δ+*tetFKH2*-31 strain revealed a modest increase in the proportion of yeast at the early times points, but after 6hr the culture contained less than 50% hyphal cells. We compared these results to the control strain SC5314 previously cultured under the same conditions, stained and counted (34). We noted that it required less than 4 hrs for the SC5314 control to reach an almost completely hyphal culture after sub-culturing into RPMI-1640 (34).

Growth curves to determine if cell growth was impaired in the modulated strain:

The observation that isolates #29 and #31 appeared to have a defect in hyphal formation led us to analyze whether the modified strains had an overall growth defect. To that end, growth curves on all five *fkh2*Δ+*tetFKH2* isolates were compared to the THE1-CIp10 strain, the derivative strain of the parent THE1 with the addition ca*URA3* inserted at the RP10 locus alleviating the uridine auxotrophy. All strains were grown overnight in 20ml of YPD in the absence of doxycycline at 30°C to maintain *FKH2* expression. Cells were then sub-cultured 1:30 into fresh YPD plus or

minus doxycycline and grown for 7hrs (Figures 11, 12, and 13). The optical density (OD_{600}) was determined at hourly intervals.

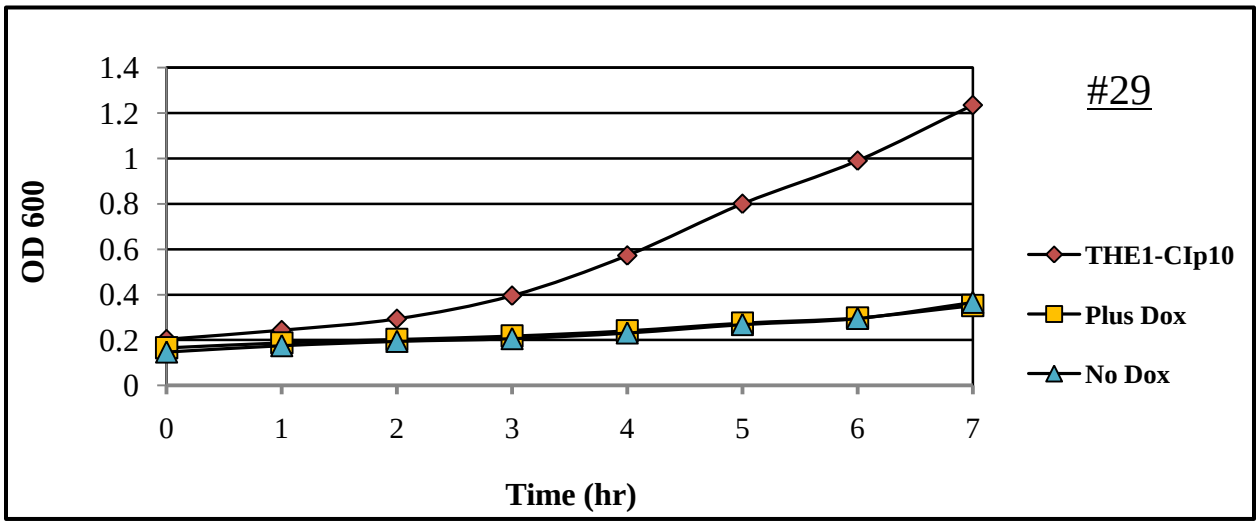

Figure 11: Growth curve of the *fkh2*Δ+*tetFKH2*-29 compared to THE1-CIp10 control.

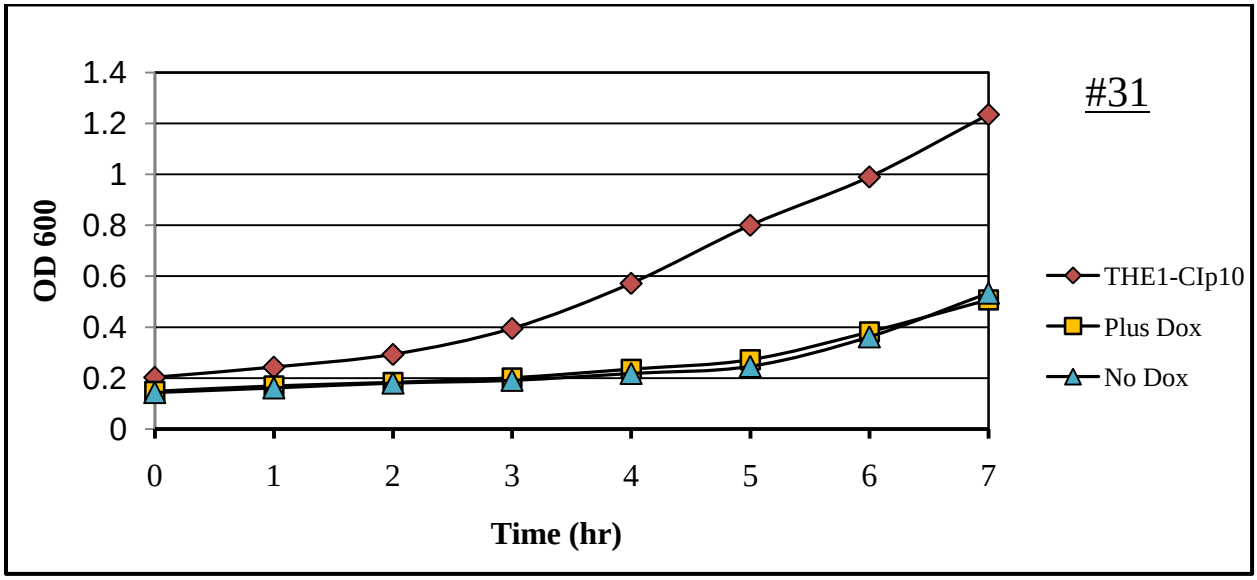

Figure 12: Growth curve of the *fkh2*Δ+*tetFKH2*-31 isolate compared to THE1-CIp10 control.

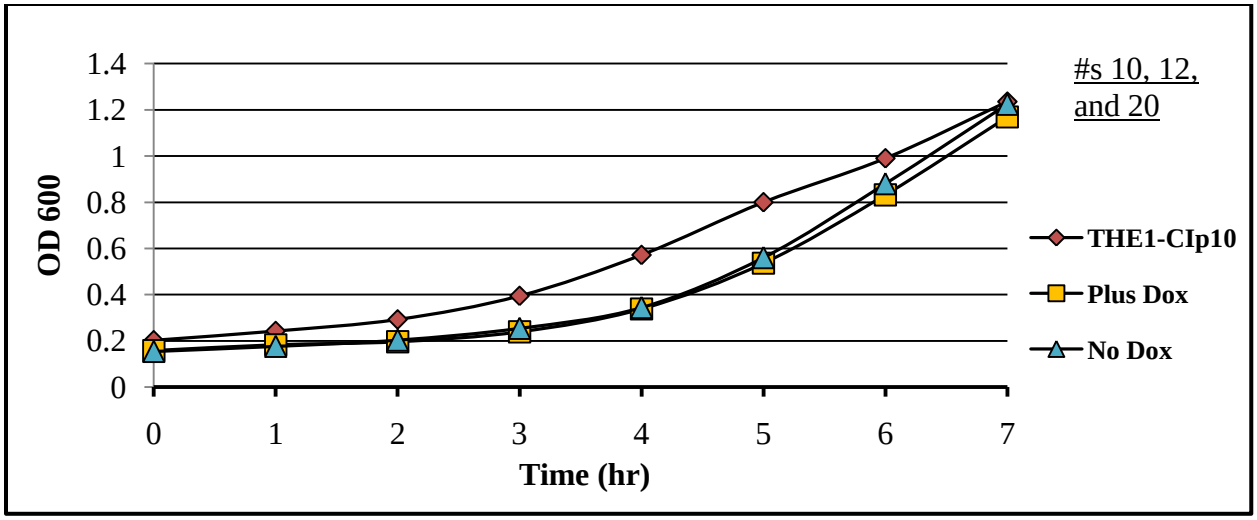

Figure 13: Growth curve of the *fkh2*Δ+*tetFKH2*-10, 12, and 20 isolates compared to the THE1-CIp10 control.

The resulting growth curves revealed that two of the five isolates, #29 and #31 grew at a much slower rate when compared to the THE1-CIp10 control (Figures 11 and 12) where as the other three (10, 12, and 20) grew at rates similar to the THE1-CIp10 strain with a small lag between the 3hr and 6hr time points (Figure 13). Based on this evidence, we concluded that the two slow growing strains #29 and #31 carry additional deleterious mutations and must be excluded from any remaining experiments. The growth curves of the three faster growing strains revealed that after 7 hours of growth there was no significant difference in growth rates based solely on the presence or absence of doxycycline. Furthermore, we concluded that the previous hyphal induction studies must be repeated using isolates 10, 12, and 20 because they were previously conducted with the two slower growing strains which apparently have other defects unrelated to the absence of *FKH2*.

In vitro analysis of the pseudohypha-to-hypha transition during the modulation of expression in strain *fkh2*Δ+*tetFKH2*-20: The faster growing isolate *fkh2*Δ+*tetFKH2*-20 was grown in YPD at 30°C overnight for 16 to 22 hours and then sub-cultured into RPMI-1640 grown at 37°C. As before, aliquots were removed at specific time-points and the cells morphology analyzed via fluorescence microscopy. Figure 13, represents the averaged percentages of the experiment performed in triplicate where the total cell count (n= 6097 cells) revealed that a starting culture consisting from 80 to 90% pseudohyphal cells induced to form hyphae took less than 4 hrs to become a more than 60% hyphal culture and that there was no increase in the yeast cell population at early time points.

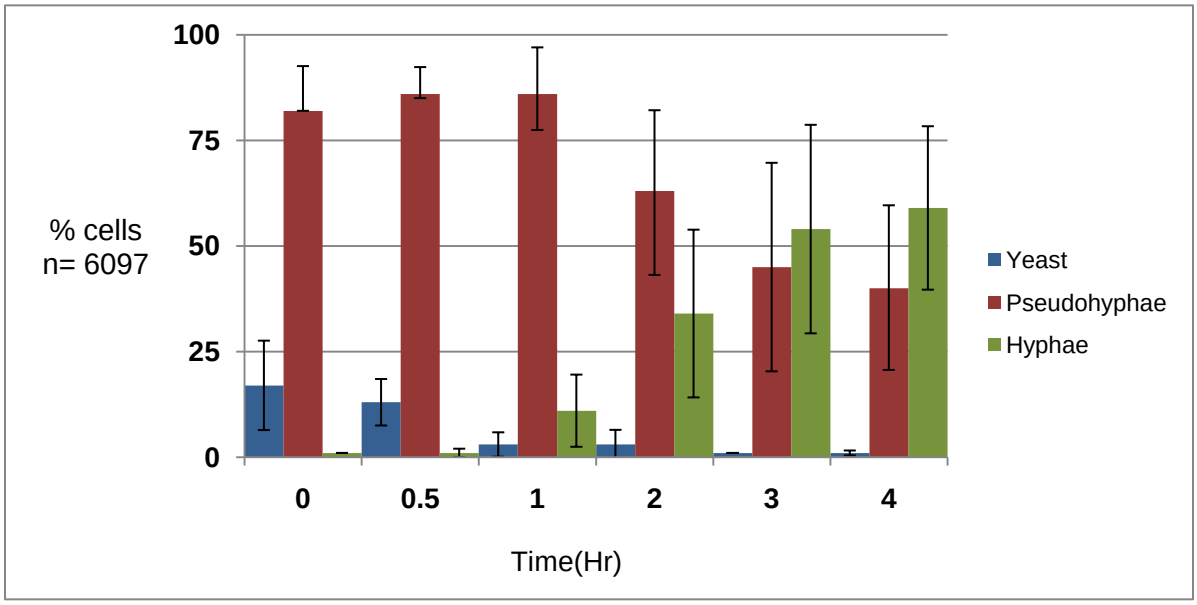

Figure 14: The *fkh2*Δ+*tetFKH2*-20 strain grown in yeast conditions for 16 to 22 hours overnight then sub-cultured into RPMI-1640 to induce hyphal formation. Note: Error bars represent the standard deviation of hyphal induction in experimental triplicate.

Upon a closer examination of the results, we observed that the proportion of pseudohyphal cells present in the starting culture before hyphal induction correlated to the length of overnight

culturing and the amount of yeast cells visualized at early time points following hyphal induction. It appeared that overnight cultures of *fkh2*Δ+*tetFKH2*-20 in the presence of doxycycline required ≥22 hrs to become ~100% pseudohyphal. This observation posed the question of whether the overnight culturing length is a direct result of the time required to fully deplete *FKH2* expression from the *tet-FKH2* allele.

Depletion of the *FKH2* transcript in the *tet*-regulatable strain: To investigate whether the level of *FKH2* transcript directly affects the amount of time required for overnight cultures to become 100% pseudohyphal, we conducted quantitative real-time PCR analysis of *FKH2* expression at various time-points. The *fkh2*Δ+*tetFKH2*-20 strain was grown overnight in 20ml of YPD liquid medium at 30°C. Two separate 29 ml YPD cultures were then inoculated with 1ml of the overnight culture (1:30 dilution) in the presence (20μg/ml) or absence of doxycycline. Cells grown in the presence of doxycycline were harvested at 4, 14, 16, 18 and 22hrs while cells grown in the absence of doxycycline for comparison were collected at 4 and 22hrs only. All quantification values are expressed relative to the overnight culture (T_0) which is set to a value of zero. Levels of *ACT1* transcription were used as an internal control to determine the relative quantification of *FKH2* mRNA levels in the presence and absence of doxycycline. At each time point, the cells from harvested aliquots were visualized microscopically and the proportion of pseudohyphae was estimated (n= ~100 cells). T_0 consisted of 100% yeast where T_{14}-T_{22} ranged from 75 to 95% pseudohyphae. These results showed that there was not a significant difference in mRNA levels between T_{14} and T_{22} in the plus doxycycline conditions and that the *FKH2* transcript level fluctuated only slightly in the minus doxycycline controls (Figure 15). This indicates that the expression of *FKH2* has apparently reached a basal point by 14 hours and the

increase in the proportions of pseudohyphal cells within the culture between 14 to 22 hours is not a consequence of diminishing *FKH2* transcript.

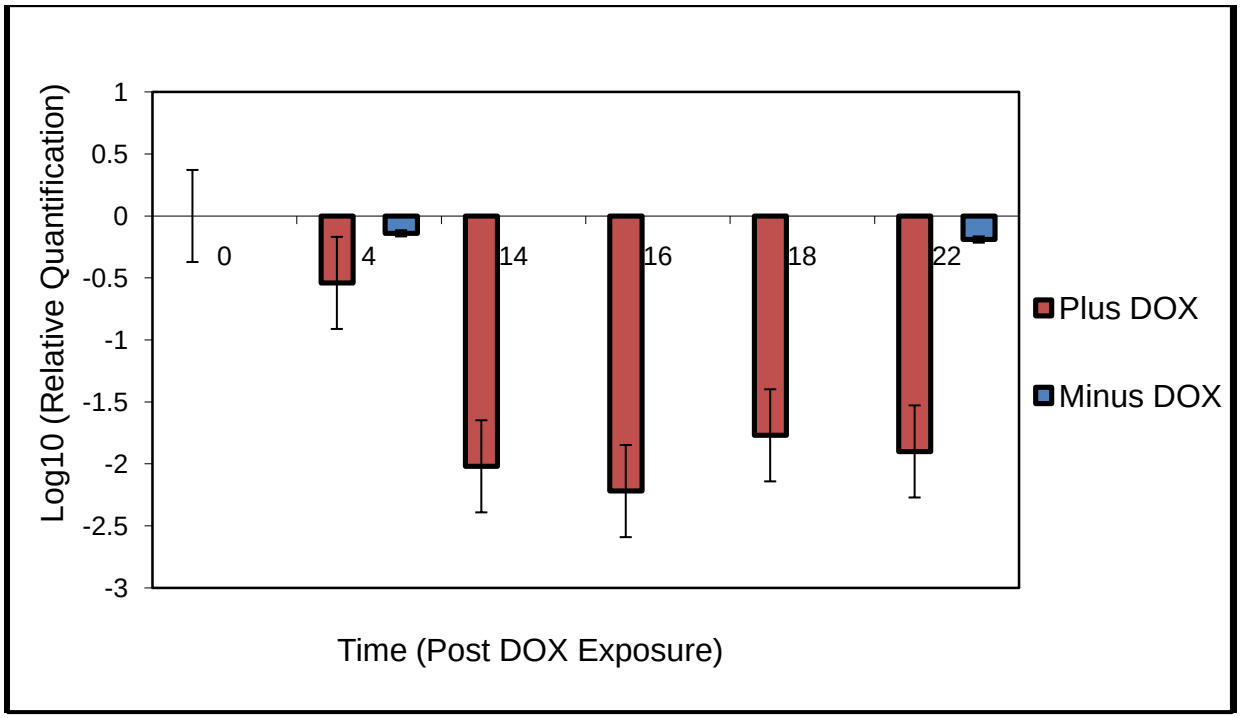

Figure 15: Quantitative real-time PCR analysis of *FKH2* expression in the *fkh2*Δ+*tetFKH2*-20 strain grown in the presence and absence of doxycycline. Note that all relative quantification values are on a log scale.

***FKH2* depleted cells show fragility during hyphal induction:**

The three faster growing *fkh2*Δ+*tetFKH2 C. albicans* isolates (10, 12, and 20) were grown overnight in the presence of doxycycline at 20μg/ml (no *FKH2* transcription). Cells were then induced to form hyphae with RPMI-1640, stained with Calcofluor White and DAPI, and visualized microscopically as before. Cells visualized at earlier time points (between 30 minutes to 2 hrs) exhibited significant cell fragility (Figure 16).

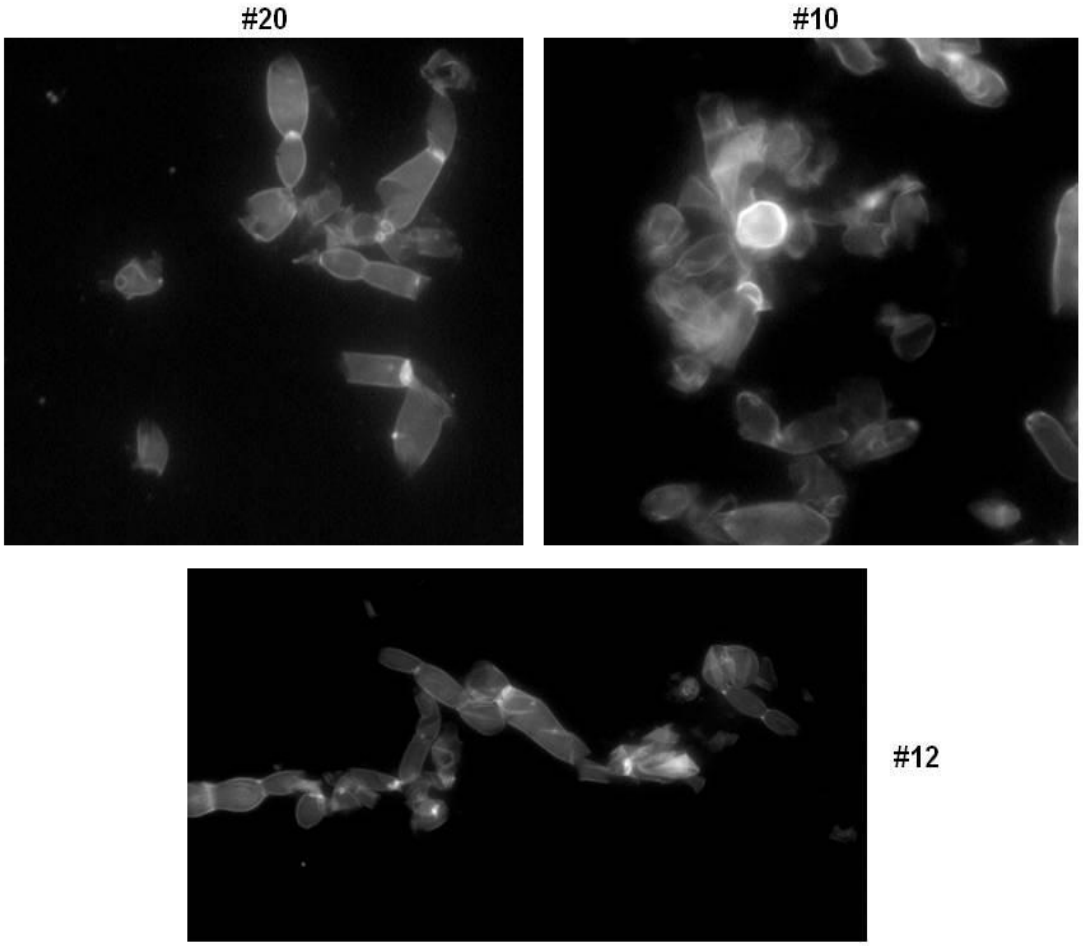

Figure 16: Notable amounts of cell bursting and cell debris observed 1hr after hyphal induction in the *fkh2*Δ+*tetFKH2* isolates #10, #12, and #20.

To further explore this fragility, we conducted sensitivity tests on the *fkh2*Δ+*tetFKH2* isolates using varying concentrations of the known cell wall-perturbing agents SDS, Congo Red, $NaCl_2$, and Calcofluor White (38). The THE1-CIp10 control and two of the *fkh2*Δ+*tetFKH2* isolates (29 and #12) were grown overnight and subsequently sub-cultured 1:20 into fresh YPD and grown at 30°C for 4 hours. The cells were harvested by centrifugation, washed and

resuspended in PBS. Cells were counted using a hemocytometer and serially diluted 6-fold from a starting solution containing 10^6cfu/ml. Aliquots (5µl-10µl) from each dilution series were spotted onto YPD plates with or without one of the following additives: SDS (0.025%), Calcofluor White (100µg/ml), Congo Red (200µg/ml), or 1M $NaCl_2$ in both the presence and absence of doxycycline (Figure 17). These tests revealed that the *fkh2*Δ+*tetFKH2*-10 and *fkh2*Δ+*tetFKH2*-12 isolates were highly sensitive to all of the perturbing agents in the presence of doxycycline, where the THE1-CIp10 control, was only sensitive to Congo Red and 0.025% SDS. Results showed that the *fkh2*Δ+*tetFKH2* isolates grown in the absence of doxycycline were more sensitive to 0.025% SDS than the control strain. The experiment was then repeated with all three *fkh2*Δ+*tetFKH2* isolates #10, #12, and #20 and the THE1-CIp10 control strain to determine whether the addition of 1M sorbitol to the 1M $NaCl_2$ plates could rescue the $NaCl_2$ sensitive phenotype. In addition, a lower SDS concentration of 0.005% was tested on all the *fkh2*Δ+*tetFKH2* isolates and the THE1-CIp10 strain to determine whether the susceptibility to SDS was merely a consequence of the high concentration used. These results revealed that the addition of sorbitol did not rescue the sensitivity to 1M $NaCl_2$ (Figure 17) and also that the *fkh2*Δ+*tetFKH2* isolates were indeed more sensitive to SDS than the THE1-CIp10 cells. We therefore concluded that the depletion of *FKH2* contributes to a previously uncharacterized loss of cell wall integrity.

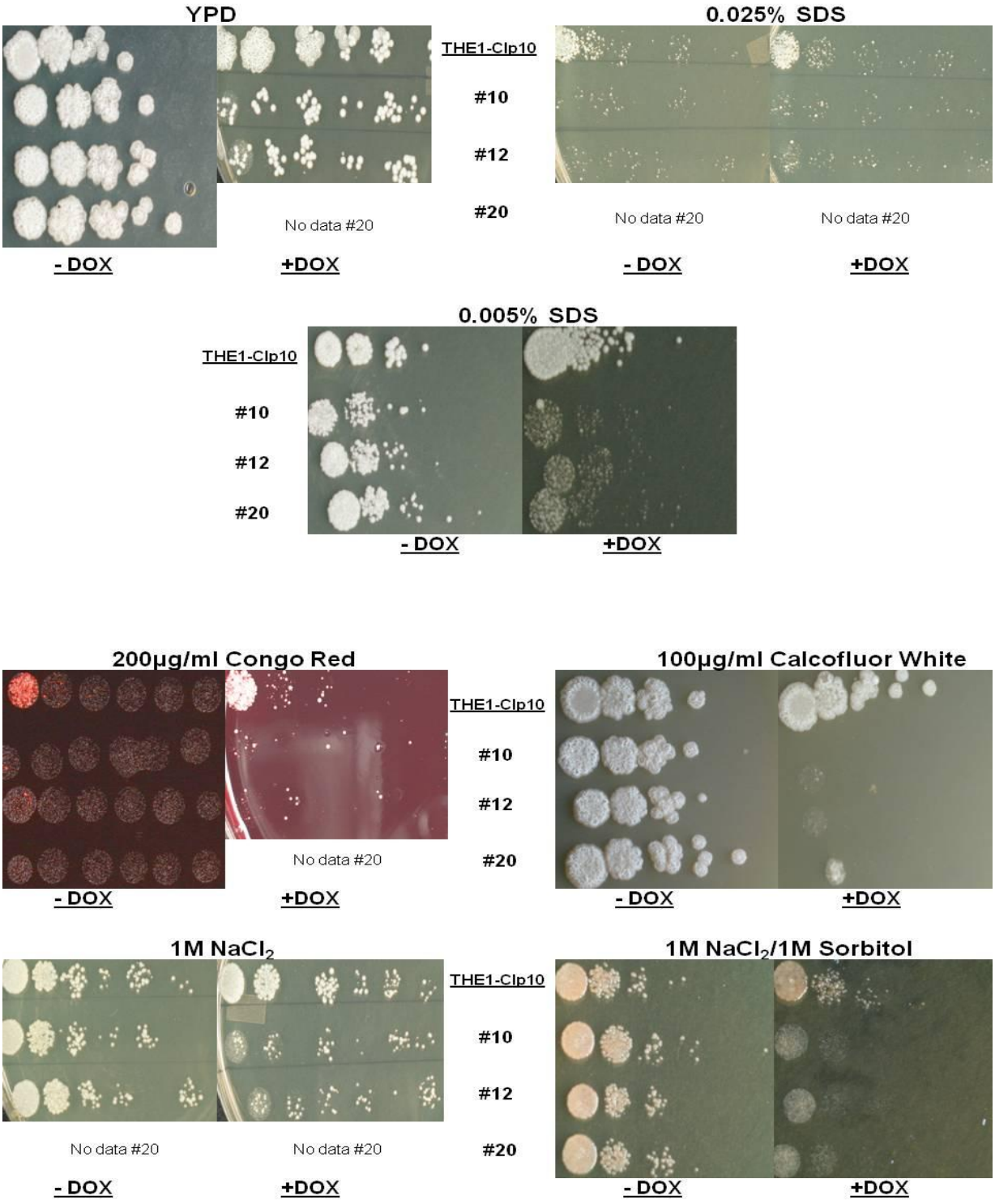

Figure 17: The *fkh2*Δ+*tetFKH2* and THE1-CIp10 strains exposed to cell wall-perturbing agents.

CHAPTER FOUR

DISCUSSION

Candida albicans is a human opportunistic pathogen. The ability of this pleiomorphic fungus to alternate cellular morphology in response to different environmental cues is believed to be a requisite virulence factor. Research on morphological transitioning mainly focuses on the yeast-to-hyphae transition. The pseudohypha-to-hypha transition remains a bit of a mystery. It is unclear whether the pseudohypha-to-hypha transition is direct. A recent review compiled by Bastidas et al. describes the importance of elucidating the pseudohypha-to-hypha transition (3). Bastidas argues that from an evolutionary stand point the *C. albicans* divergence from the non-pathogenic fungus *S. cerevisiae* more than 200 million years ago could have been the turning point in which the pseudohypha of *S. cerevisiae* began expanding its filamentous repertoire. This expansion to the much more elongated hyphal morphology allowed for more efficient nutrient foraging. This connection in evolution from relatively harmless to pathogenic species sheds light on the diverging molecular circuitries that direct pathogenesis. The more we understand of the selective pressures that drive genetic variation in these circuits between species the closer we shall be to treating the potentially dangerous infections they cause.

Morphologic transitioning is tightly regulated by the *tet*O-promoter in the *fkh2*Δ+*tetFKH2* strain: The absence of *FKH2* in *Candida albicans* confers a constitutive pseudohyphal phenotype under all growth conditions. The cells of a null mutant are unable to transition to yeast or hyphal morphologies and grow with a uni-polar budding pattern with characteristic constrictions at all septal junctions (4). This constitutive pseudohyphal phenotype provided a perfect opportunity to explore the pseudohypha-to-hypha transition by modulating *FKH2*

expression. Integrating the *tet*O-*FKH2* allele into a THE1- *fkh2*Δ parent strain enabled such modulation using the tetracycline-regulatable (TR) system (30). THE1 carries the TR transactivator (*Tet*R-ScHAP4AD) inserted at the *ENO1* locus (30). This transactivator gene is a fusion protein consisting of two well characterized sequences; the DNA binding domain of *Tet*R, the *Escherichia coli* tetracycline repressor protein and *HAP4AD*, the activation domain of the *Saccharomyces cerevisiae* Hap4p transcription factor. Codon corrections have been made at four locations within the fusion protein to ensure proper function in *C. albicans* which translates CUG as serine instead of leucine (30). The highly specific binding of *tet*R to the *tet*O sequence allows the high fold induction of the *FKH2* gene when doxycycline (a small molecule tetracycline derivative) is added *in vitro* or *in vivo*. Doxycycline binds to *tet*R thereby preventing dimerization at *tet*O and effectively shuts off the expression of the proceeding *FKH2*. The *fkh2*Δ+*tetFKH2* strains #10, #12, and #20 produced in this study grew like wild-type *Candida albicans* SC5314 in the absence of doxycycline under all growth conditions.

***In vitro* analysis revealed that *FKH2* depleted pseudohyphae do not revert to yeast before transitioning to hyphae:** The results from our *in vitro* analysis demonstrated that the constitutive pseudohyphae produced by the *fkh2*Δ+*tetFKH2* strains did not have to revert to yeast before transitioning to hyphae. Unlike the *tet-RFG1* strain in which the pseudohyphae revert to yeast before transitioning to hyphae, the *FKH2* depleted pseudohyphae appear to directly transition to hyphae. This continuum contradicts the previous studies which suggest that the three principal morphologies are distinct fates in *Candida albicans*. The pseudohyphae exhibited hyper uni-polarized growth upon hyphal induction resulting in cells with hybrid-like morphology consisting of pseudohyphal cells with constricted septa connected to hyphal cells with no septal

constrictions (Figure 18). The small percentage of budded yeast in the starting culture appeared to form normal hyphal cells with no constrictions at the mother-daughter bud neck during all time points.

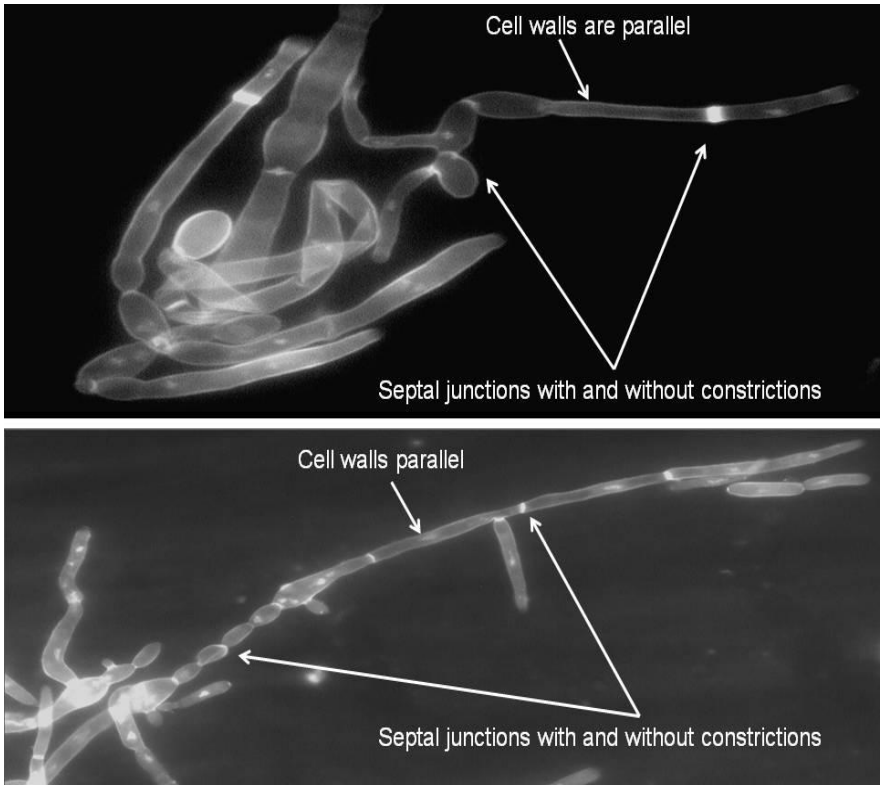

Figure 18: Hybrid-like morphology produced during *in vitro* hyphal induction experiments indicating a direct transition from the pseudohyphal to a hyphal morphology.

Similarly, to the conflicting stimuli seen when *tet-RFG1* pseudohyphae were placed in hypha inducing medium these results could be a product of mixed signals. If as posited, Fkh2*p* operates as a repressor of pseudohyphal growth (4), this function may be absent from the *fkh2*Δ*/tet-FKH2* cells at early time-points until normal Fkh2p levels are restored. Consistent with this, the hyphal elements always appear at the distal ends of the chains.

Real-time PCR analysis reveals that the depletion of the *FKH2* transcript does not directly correlate with the proportion of pseudohyphae in overnight cultures: Quantitative, real-time PCR analysis conducted on cDNA synthesized from the *fkh2*Δ+*tetFKH2*-20 strain shows that the *FKH2* transcript is depleted after growth in YPD at 30°C in the presence of doxycycline for 14 hours. The proportion of pseudohyphal cells within the culture at T_{14} were ~75% which indicates that the absence of the *FKH2* transcript is not directly related to pseudohyphal population once the transcript is fully repressed since the percentage of these cells continues to rise until 20 to 22 hours. These results could indicate that Fkh2p is highly stable. Also, the *tetFKH2* allele at the RP10 locus over-expresses *FKH2* which could potentially result in excess Fkh2p levels requiring an extended period of time to degrade. This combination of the overproduction of Fkh2p and its presumed stability could delay its depletion lengthening the time required to produce a 100% pseudohyphal culture. To further explore these two theories, future experimentation is necessary.

Sensitivity assays confirm that the depletion of the *FKH2* transcript contributes to cell wall fragility: The degree of cell bursting and the associated cell debris visualized in the *fkh2*Δ+*tetFKH2* strain grown in the presence of doxycycline is highly unusual in *C. albicans* due to the cell wall tensile strength afforded by chitin, a β(1,4)-homopolymer of *N*-acetylglucosamine, and β(1-3) glucan (29). Sensitivity to cell wall-perturbing agents has been documented in experiments analyzing genes in *C. albicans* strains with defects in transcriptional regulatory networks (22). Specifically, experiments involving the disruption of genes in the RAM network which regulate the transcription of Ace2p, a transcription factor involved in

polarized morphogenesis, show defects in morphogenesis, cell polarity and cell separation following cytokinesis (38). These RAM network phenotypes all resemble those observed in the *FKH2* modulated strain. *C. albicans* Ace2p is also believed to regulate genes necessary for ergosterol biosynthesis and cell wall remodeling during morphogenesis (28). As previously stated, Fkh2p in *S. cerevisiae* regulates transcription of *ACE2* and some of its downstream targets such as the endochitinases that are up-regulated in yeast cells. The *fkh2*Δ+*tetFKH2* mutants (plus doxycycline) showed sensitivity to all cell wall-perturbing agents tested and the addition of sorbitol, an organic osmolyte which cells take up as a stress response in order to maintain isosmolarity, did not improve this sensitivity (39). Interestingly, a recent study showed that an *ace*2Δ mutant displayed enhanced growth when subjected to Calcofluor White indicating that the Fkh2p does not directly regulate *ACE2* in *C. albicans* (22). Conversely, experiments by Song et al. analyzing null mutants of several *ACE2* downstream targets such as; *MOB1*, *CBK1*, *KIC1*, *HYM1*, and *SOG2* showed that all were highly sensitive to Calcofluor White though, cell growth was rescued slightly by the addition of sorbitol (38). At this point there is no direct evidence linking *FKH2* and *ACE2* in *C. albicans*, but future microarray or quantitative real-time PCR analysis of the genes involved in these regulatory networks during the modulation of the Fkh2p expression could explain these confusing results.

Multi-nucleated cells were visualized in the *fkh2*Δ+*tet-FKH2* strain: The previous study characterizing the function of the *C. albicans FKH2* gene conducted by Bensen et al., carried out microscopic visualization techniques similar to ours by using Calcofluor White for septin and DAPI for nuclear staining (5). During our analysis of the pseudohyphal-to-hyphal transition we observed cells with multiple nuclei in all the *fkh2*Δ+*tetFKH2* strains grown in the presence of

doxycycline (Figure 19). The Bensen study did not indicate the appearance of cells with multiple nuclei. What is unusual about this observation is that upon hyphal induction in the absence of doxycycline *FKH2* expression is restored. Fkh2p should then be present to negatively regulate *CLB4* allowing for its degradation and the cells should properly exit mitosis. During the characterization study of the Clb4p, it was noted that upon hyphal induction the levels of Clb4p is low and that cells with elevated Clb4p upon hyphal induction fail to exhibit hyperpolarized growth (5). The accumulation of Clb4p at high levels before hyphal induction in Fkh2p depleted cells could contribute to the multi-nucleated phenomenon we observed. Also, it is important to note that disruptions in the RAM network can also lead to multi-nucleated phenotypes (38).

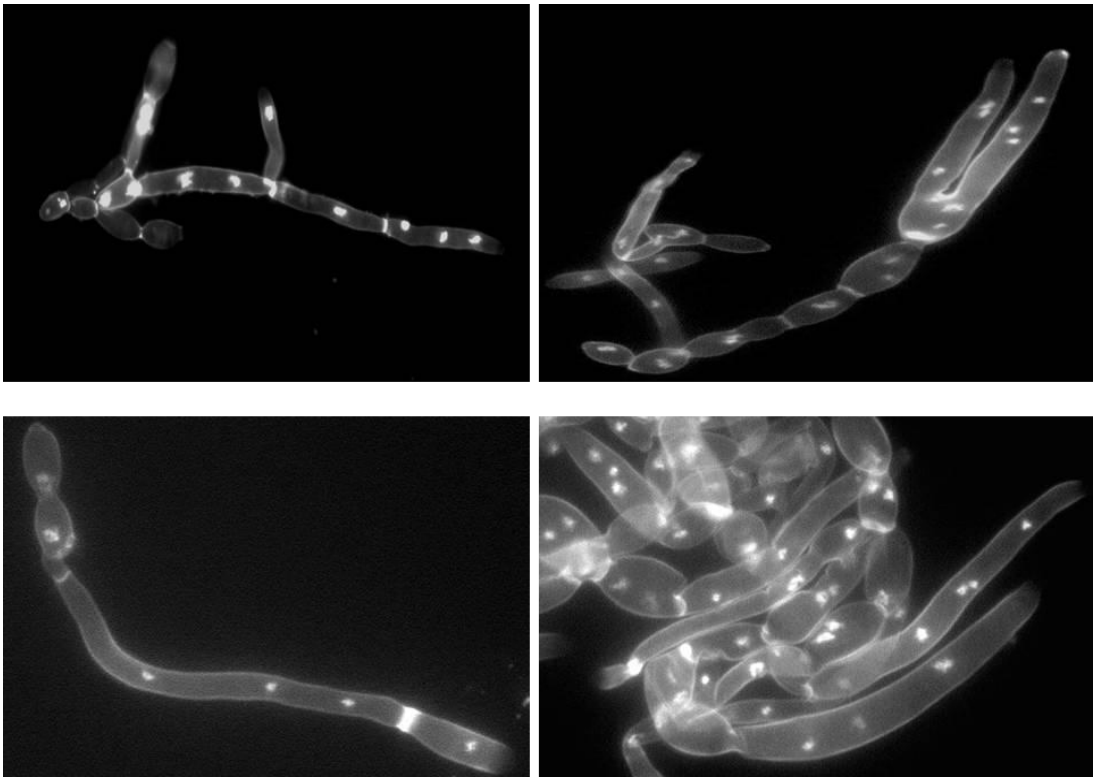

Figure 19: Multi-nucleated cells visualized in the *fkh2*Δ+*tetFKH2* strains.

To explore this phenomenon further while at the same time observing the pseudohypha-to-hypha direct transition, we began creating GFP-fusion constructs to enable us to visualize *CDC3* and *NOP1* in the *fkh2*Δ+*tetFKH2*-20 strain. Cdc3p is a septin which localizes to the site of septation in yeast and filamentous morphologies and Nop1p is a small nucleolar ribonucleoprotein (17). These two genes have been successfully tagged and visualized previously in *C. albicans* (17). *Fkh2*Δ+*tetFKH2* strains containing the *CDC3* and *NOP1* GFP-fusions will give us the ability to capture time-lapse images *in vivo* during nuclear division and the formation of septin rings. Cassettes designed by Gerami-Nejad et al. allow the downstream fusion of the GFP gene to a desired target gene by PCR-mediated tagging (19). The original GFP cassette includes the *HIS1* gene for transformant selection which is unsuitable for use in the *fkh2*Δ+*tetFKH2* strains. We therefore replaced this with the *SAT1* gene for nourseothricin selection (Figure 20). The primers and plasmids to be used in the GFP-fusion construction are listed in Table 2 and Table 3. Unfortunately, at this time we have been unsuccessful in our attempts to tag *CDC3* and *NOP1* with GFP in the *fkh2*Δ+*tetFKH2*-20 strain.

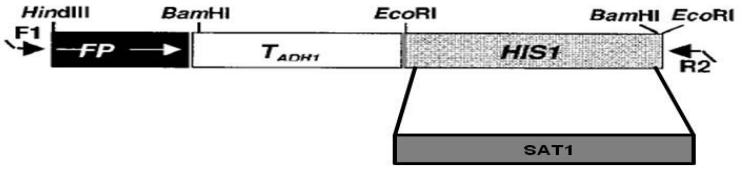

Figure 20: The GFP-Cassette showing the replacement of *HIS1* with *SAT1* through restriction enzyme digestion and ligation (19).

Conclusions:

The production of the novel *fkh2*Δ+*tetFKH2* provides further evidence on the pseudohyphal-to-hyphal transition in *Candida albicans*. To summarize:

1. The *fkh2*Δ+*tetFKH2* strain produces constitutive pseudohyphae in the presence of doxycycline.
2. The pseudohyphal-to-hyphal transition is a continuum during the manipulation of *FKH2* expression.
3. The absence of Fkh2p causes cell wall fragility and sensitivity to cell wall-perturbing agents during hyphal induction.
4. The absence of the Fkh2p leads to multi-nucleated cells during hyphal induction.

Bibliography

1. **Achkar, J. M., and B. C. Fries**. 2010. Candida Infections of the Genitourinary Tract. Clinical Microbiology Reviews **April**:253–273.
2. **Banerjee, M., D. S. Thompson, A. Lazzell, P. L. Carlisle, C. Pierce, C. Monteagudo, J. L. Lopez-Ribot, and, and D. Kadosh**. 2008. UME6, a Novel Filament-specific Regulator of Candida albicans Hyphal Extension and Virulence. Molecular Biology of the Cell **19**:1354–1365.
3. **Bastidas, J. R., and J. Heitman**. 2009 Trimorphic stepping stones pave the way to fungal virulence. PNAS **106**:351–352.
4. **Bensen, E., J. Berman, and S. G. Filler , and** 2002. A Forkhead transcription factor is important for true hyphal as well as Yeast morphologies in Candida albicans. Eukaryotic Cell **1**:787-798.
5. **Bensen, E. S., A. Clemente-Blanco, K. R. Finley, J. Correa-Bordes, and J. Berman**. 2005. The Mitotic Cyclins Clb2p and Clb4p Affect Morphogenesis in Candida albicans. Molecular Biology of the Cell **16**:3387–3400.
6. **Benson, E., J. Berman, and S. G. Filler , and** 2002. A Forkhead transcription factor is important for true hyphal as well as Yeast morphologies in Candida albicans. Eukaryotic Cell **1**:787-798.
7. **Berman, J.** 2006. Morphogenesis and cell cycle progression in Candida albicans. Current Opinion Microbiology **9**:595-601.
8. **Berman, J., and P. E. Sudbery**. 2002. Candida albicans: A Molecular Revolution Built On Lessons From Budding Yeast. Nature **3**:918-930.
9. **Bernard, F., A. Bruno**. 2001. Ubiquitin and the SCF(Grr1) ubiquitin ligase complex are involved in the signalling pathway activated by external amino acids in Saccharomyces cerevisiae. FEBS Letters **496**:81-85.
10. **Bernardo, S. M., Z. Khalique, J. Kot, J. K. Jones, and S. A. Lee**. 2008. Candida albicans VPS1 contributes to protease secretion, filamentation, and biofilm formation. Fungal Genet Biol. **45**:861–877.

11. **Carlisle, P., M. Banerjee, A. Lazzell, C. Monteagudo, J. Lopez-Ribot, and D. Kadosh** 2009. Expression levels of a filament-specific transcriptional regulator are sufficient to determine Candida albicans morphology and virulence. PNAS **6**:599-604.
12. **Cleary, I. A., P. Mulabagal, S. M. Reinhard, D. P. Thomas, and S. P. Saville**. 2010. Pseudohyphal Regulation by the Transcription Factor Rfg1p in Candida albicans Eukaryotic Cell **9**:1363-1373.
13. **Côte, P., H. Hogues, and M. Whiteway**. 2009. Transcriptional Analysis of the Candida albicans Cell Cycle. Molecular Biology of the Cell **20** 3363–3373.
14. **Crampin, H., K. Finley, M. Gerami-Nejad, H. Court, C. Gale, J. Berman, and P. Sudbery**. 2005. Candida albicans hyphae have a Spitzenkorper that is distinct from the polarisome found in yeast and pseudohyphae. Journal of Cell Science **118**:2935-2947.
15. **Dohrmann, P. R., G. Butler, K. Tamai, S. Dorland, J. R. Greene, D. J. Thiele, and D. J. Stillman** 1992. Parallel pathways of gene regulation: homologous regulators SWI5 and ACE2 differentially control transcription of HO and chitinase. Genes and Development **6**:93-104.
16. **Edmond, M. B., S. E. Wallace, D. K. McClish, M. A. Pfaller, R. N. Jones, and R. P. Wenzel**. 1999. Nosocomial Bloodstream Infections in United States Hospitals: A Three-Year Analysis. Clinical Infectious Diseases **29**:239–244.
17. **Finley, K. R., and J. Berman**. 2005. Microtubules in Candida albicans Hyphae Drive Nuclear Dynamics and Connect Cell Cycle Progression to Morphogenesis. Eukaryotic Cell **4**:1697–1711.
18. **Foxman, B., R. Barlow, H. D'Arcy, B. Gillespie, and J. D. Sobel** 2000. Candida vaginitis—self-reported incidence and associated costs. SexuallyTransmitted Disease **27**:230-235.
19. **Gerami-Nejad, M., J. Berman, and C. Gale**. 2001. Cassettes for PCR-mediated construction of green, yellow, and cyan fluorescent protein fusions in Candida albicans. Yeast **18**:859-864.
20. **Gillum, A. M., E. Y. Tsay, and D. R. Kirsch** 1984. Isolation of the Candida albicans gene for orotidine-5-phosphate decarboxylase by complementation of S. cerevisiae ura3 and E. coli pyrF mutations. Molecular Gen. Genet. **198**:179–182.

21. **Hazan, I., M. Sepulveda-Becerra, and H. Liu**. 2002. Hyphal Elongation Is Regulated Independently of Cell Cycle in Candida albicans. Molecular Biology of the Cell **13**:134–145.
22. **Homann, O. R., J. Dea, S. M. Noble, A. D. Johnson**. 2009. A Phenotypic Profile of the Candida albicans Regulatory Network. PLoS Genetics **5**:e1000783.
23. **King, L., and G. Butler**. 1998. Ace2p, a regulator of CTS1 (chitinase) expression, affects pseudohyphal production in Saccharomyces cerevisiae. Current Genetics **34**:183–191.
24. **Klein, B. S., and B. Tebbets** 2007. Dimorphism and virulence in fungi. Current Opinion Microbiology **10**:1-6.
25. **Lavoie, H., H. Hogues, J. Mallick, A. Sellam, A. Nantel, and M., and Whiteway**. 2010. Evolutionary Tinkering with Conserved Components of aTranscriptional Regulatory Network. PLos Biology **8**:e1000329.
26. **Lo, H. J., J. R. Kohler, and B. DiDomenico**. 1997. Nonfilamentous C. albicans Mutants Are Avirulent. Cell **90**:939-949.
27. **Merson-Davies, L. A., and F. C . Odds**. 1989. A Morphology Index for Characterization of Cell Shape in Candda albicans. Journal of General Microbiology **135**:3143-3152.
28. **Mulhern, S. M., M. E. Logue, and G. Butler**. 2006. Candida albicans Transcription Factor Ace2 Regulates Metabolism and Is Required for Filamentation in Hypoxic Conditions. Eukaryotic Cell **5**:2001–2013.
29. **Munro, C. A., K. Rhian, H. Whitton, B. Hughes, M. Rella, S. Selvaggini, and N. Gow**. 2003. CHS8—a fourth chitin synthase gene of Candida albicans contributes to in vitro chitin synthase activity, but is dispensable for growth. Fung. Genet. and Bio **40**:146-158.
30. **Nakayama, H., T. Mio, S. Nagahashi, M. Kokado, M. Arisawa, and Y. Aoki**. 2000. Tetracycline-regulatable system to tightly control gene expression in the pathogenic fungus Candida albicans. Infect. and Immunity **68**:6712-6719.
31. **Paget, M. S., G. Hintermann, and C. P. Smith**. 1994. Construction and application of streptomycete promoter probe vectors which employ the Streptomyces glaucescens tyrosinase-encoding gene as reporter. Gene **146**:105-110.
32. **Pappas, P. G., J. Rex, J. Lee, R. J. Hamill, W, and E. Dismukes** 2003. A Prospective Observational Study of Candidemia: Epidemiology, Therapy, and Influences on Mortality in Hospitalized Adult and Pediatric Patients. Clinic. Infect. Disease **37**:634-643.

33. **Pic, A., F.-L. Lim, S. J. Ross, E. A. Veal, M. R.A. Sultan, A. G. West, and B. A. Morgan et al.** 2000. The forkhead protein Fkh2 is a component of the yeast cell cycle transcription factor SFF. EMBO **19**:3750-3761.
34. **Prasad, D., S. P. Saville**. 2008. Unpublished Study Report.
35. **Reuss, O., A. Vik, R. Kolter, and J. Morschhauser**. 2004. The SAT1 flipper, an optimized tool for gene disruption in Candida albicans. Gene **341**:119-127.
36. **Saville, S. P., A. L. Lazzell, C. Monteagudo, and J. L. Lopez-Ribot**. 2003. Engineered Control of Cell Morphology In Vivo Reveals Distinct Roles for Yeast and Filamentous Forms of Candida albicans during Infection. Eukaryotic Cell **2**:1053–1060.
37. **Soll, D. R., M. A. Herman, M. A. Staebell**. 1985. The involvement of cell wall expansion in the two modes of mycelium formation of Candida albicans. . J. Gen. Microbiol. **131**:2367-2375.
38. **Song, Y., A. S. Cheon, K. E. Lee, Son Lee, B-K. Lee, D-B. Oh, H. A. Kang, and J-Y. Kim** 2008. Role of the RAM Network in Cell Polarity and Hyphal Morphogenesis in Candida Albicans. Molecular Biology Cell **19**:5456-5477.
39. **Strange, K.** 2004. Cellular volume homeostasis. Advances in Physiology Education **28**:155-159.
40. **Sudbery, P., N. Gow, and J. Berman**. 2004. The Distinct Morphogenic States of Candida albicans. Trends in Microbiology **12**:317-324.
41. **Thompson, J. R., E. Register, J. Curotto, M. Kurtz, and R. Kelly**. 1998. An Improved Protocol for the Preparation of Yeast Cells for Transformation by Electroporation. Yeast **14**:565–571.
42. **Toyoda, M., T. Cho, H. Kaminishi, M. Sudoh, and H. Chibana**. 2004. Transcriptional profiling of the early stages of germination in Candida albicans by real-time RT-PCR. FEMS Yeast Res. **5**:287-296.
43. **Umeyama, T., A. Kaneko, M. Niimi, Y. Uehara**. 2006. Repression of CDC28 reduces the expression of the morphology-related transcription factors, Efg1p, Nrg1p, Rbf1p, Rim101p, Fkh2p and Tec1p and induces cell elongation in Candida albicans. . Yeast **23**:537-552.
44. **Umeyama, T., A. Kaneko, Y. Nagai, N. Hanaoka, K. Tanabe, Y. Takano, M. Niimi, and Y. Uehara**. 2005. Candida albicans protein kinase CaHsl1p regulates cell elongation and virulence. Molecular Microbiology **55**:381–395.

45. **Veses, V., and N. A. R. Gow**. 2009. Pseudohypha budding patterns of Candida albicans. Medical Mycology **47**:268-275.
46. **Wightman, R., S. Bates, P. Amornrrattanapan, and P. Sudbery**. 2004. In Candida albicans, the Nim1 kinases Gin4 and Hsl1 negatively regulate pseudohypha formation and Gin4 also controls septin organization. The Journal of Cell Biology **164** 581–591.

VITA

I am originally from Longview, Texas (population 78,000). I graduated from Longview High School in 1994 and moved to Austin, Texas to attend The University of Texas. I graduated in 1998 with a BFA focusing in metalsmithing. I worked in metal and art for 8 years, as an industrial jeweler in New York City and as a self-employed artist and gallery-owner in Austin from 2003 to 2006. I returned to school in 2006 and attended Austin Community College to earn an Associate's Degree in Biotechnology. My mentor at A.C.C., Dr. Patricia Phelps, suggested I attend graduate school for biotechnology at The University of Texas at San Antonio. My father Charles is a retired electrical contractor holding a BA in Psychology; my mother Elizabeth is a retired registered nurse holding a BS in Nursing; my sister May is a published author holding an MA in Literature, my sister Beth is the mother of two insanely-adorable twin boys and holds a BS in Mechanical Engineering and an MS in Physics; and my husband David is an accomplished musician and improvisational comedian with BA degrees in Philosophy, History, and English, and an MS in Organizational Communication.